

Long-term Global Solar Activities Studied by the Nobeyama Radioheliograph

Kiyoto Shibasaki
Nobeyama Solar Radio Observatory

<http://solar.nro.nao.ac.jp>
shibasaki.kiyoto@nao.ac.jp

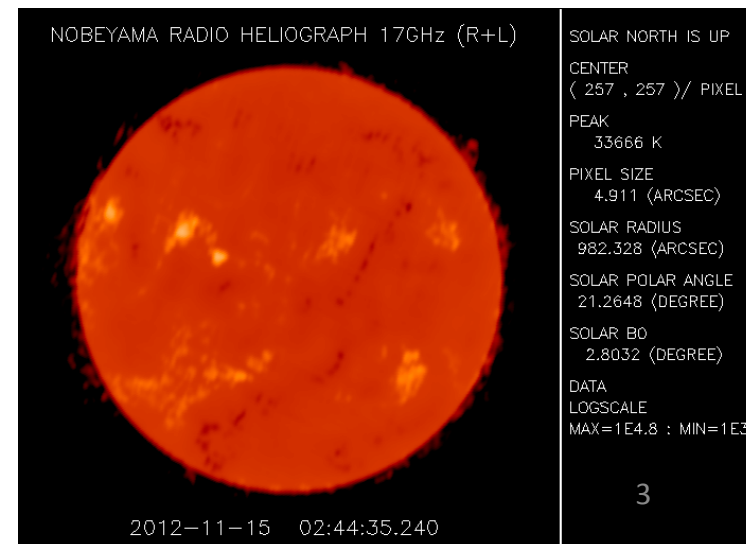
Outline

1. Nobeyama Radioheliograph (NoRH)
2. NoRH design and quiet sun studies
3. Radio features of the quiet sun and their emission mechanisms
4. Synthesis of butterfly diagram
5. Global solar activity studies by NoRH
6. Why polar regions are bright in microwaves
7. Summary

Nobeyama Radioheliograph (NoRH)

<http://solar.nro.nao.ac.jp/norh/>

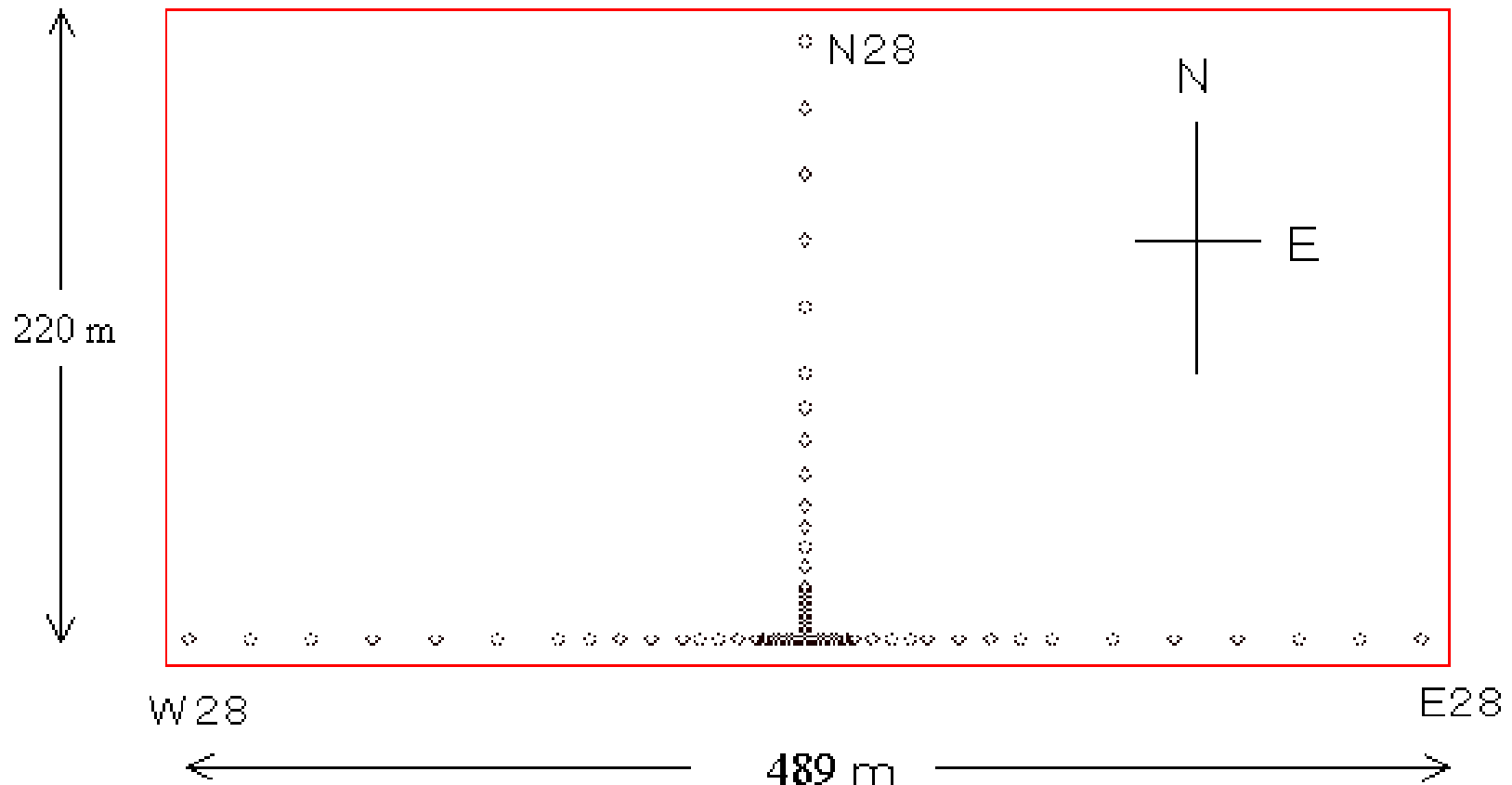
- Specification
 - 84 elements of 80 cm dishes
 - EW: 490 m, NS: 220 m
 - full disk
 - 17 GHz (I & V) and 34 GHz (I)
 - 10 / 5 arcsec (17/34 GHz) res.
 - 1 second cadence
 - 0.1 cadence during flares
- Operation
 - 1992.6 ~
 - daily 8 hr (Local noon 03UT +/- 4h)
 - Full automatic operation
 - Images around local noon and every 10 min. are on the WEB



Design Principles of NoRH

- Major science targets
 - studies of particle acceleration in solar flares
 - 17 & 34 GHz (higher than turnover frequency), high cadence (1 or 0.1 sec), full disk
- Characteristics of solar radio emission
 - Strong signal and fast variation
 - room temperature receivers (no calibrator sources are available)
 - one-bit correlator (amplitude independent correlation)
 - Complex sources (extended ~ compact)
 - Dense array: Large flux from an extended disk
+ sparse array: compact burst components
 - Observing condition is worse due to daytime obs. (turbulent atmosphere)
 - redundant array configuration: self calibration of visibilities
The Sun is the calibrator source. Each data set contains calibration data.
 - high quality images of the disk: positional and brightness reference (calibration)
 - Large number of images are needed to study dynamics
 - UV gridding should be avoided due to limited computer power (~20 years ago)

NoRH Array Configuration



The design principles fit well to QS & AR studies

- Well observed quiet Sun disk : good for studies of global solar activity
 - High quality images due to good visibility (phase and amplitude) calibration
 - Robust positional and brightness calibration
 - 17 GHz turned out to be a good frequency to study global solar activity (polar brightening + active regions)
 - High cadence observation capability allow oscillation studies of active regions (umbral 3 min. oscillation, AR oscillation)
- + Steady operation (99.4% availability) due to good design and maintenance.
- Long term (20 years) activity study is possible.

(Scientists tend to improve instruments, hence long-term uniform dataset is not easy to get. To study activities of targets, observing instruments should not be changed much.)

Radio emission from the Quiet (non-flaring) Sun

- Emission mechanisms
 - mainly thermal emission (thermal electrons)
 - free-free emission
 - gyro-resonance emission
 - simple mechanism (classical EM), electrons are in LTE state, continuum emission: DEM measurements are not possible
 - small contribution from non-thermal emission (small flares)
- Features
 - solar disk
 - active regions
 - dark filaments / prominences
 - coronal holes
 - network and fine structures (high spatial resolution, ALMA?)

$$T_b = \int T e^{-\tau} d\tau$$

QS and AR studies

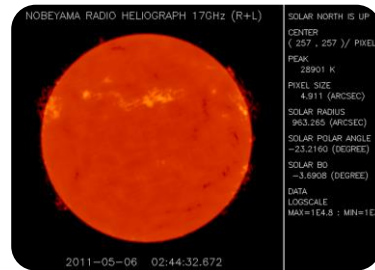
- Solar Disk
 - center-to-limb brightness variation / limb brightening
 - atmosphere model (stratified atmosphere + spicules, coronal and chromospheric heating)
 - polar brightening
 - limb brightening + coronal hole + polar mag. field activity
 - solar rotation rate
 - oscillations in quiet area
- Coronal Hole
 - on disk: partly bright area
 - enhanced limb brightening / polar brightening
- Prominence / Dark filaments
 - filament eruption / CME
- Active Regions
 - hot and dense plasma trapped by active region closed magnetic field
 - gyro-resonance: sunspot magnetic field
 - umbral oscillation (3 min. oscillation and its cycle dependence)
 - longer period oscillation (50 – 100 min. oscillation)

Long-term Global Solar Activities Inferred from Microwave Observation

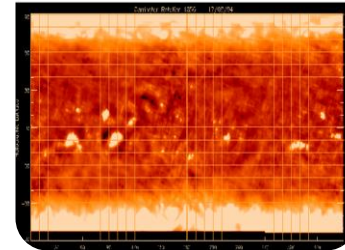
Synthesis of Radio Butterfly Diagram



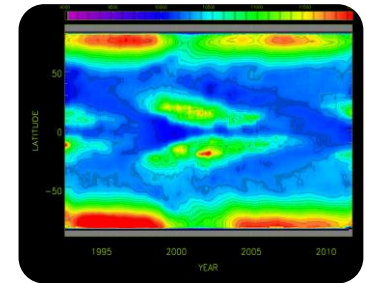
Nobeyama
Radioheliograph
Observation Since
1992



Daily Images
(7000)

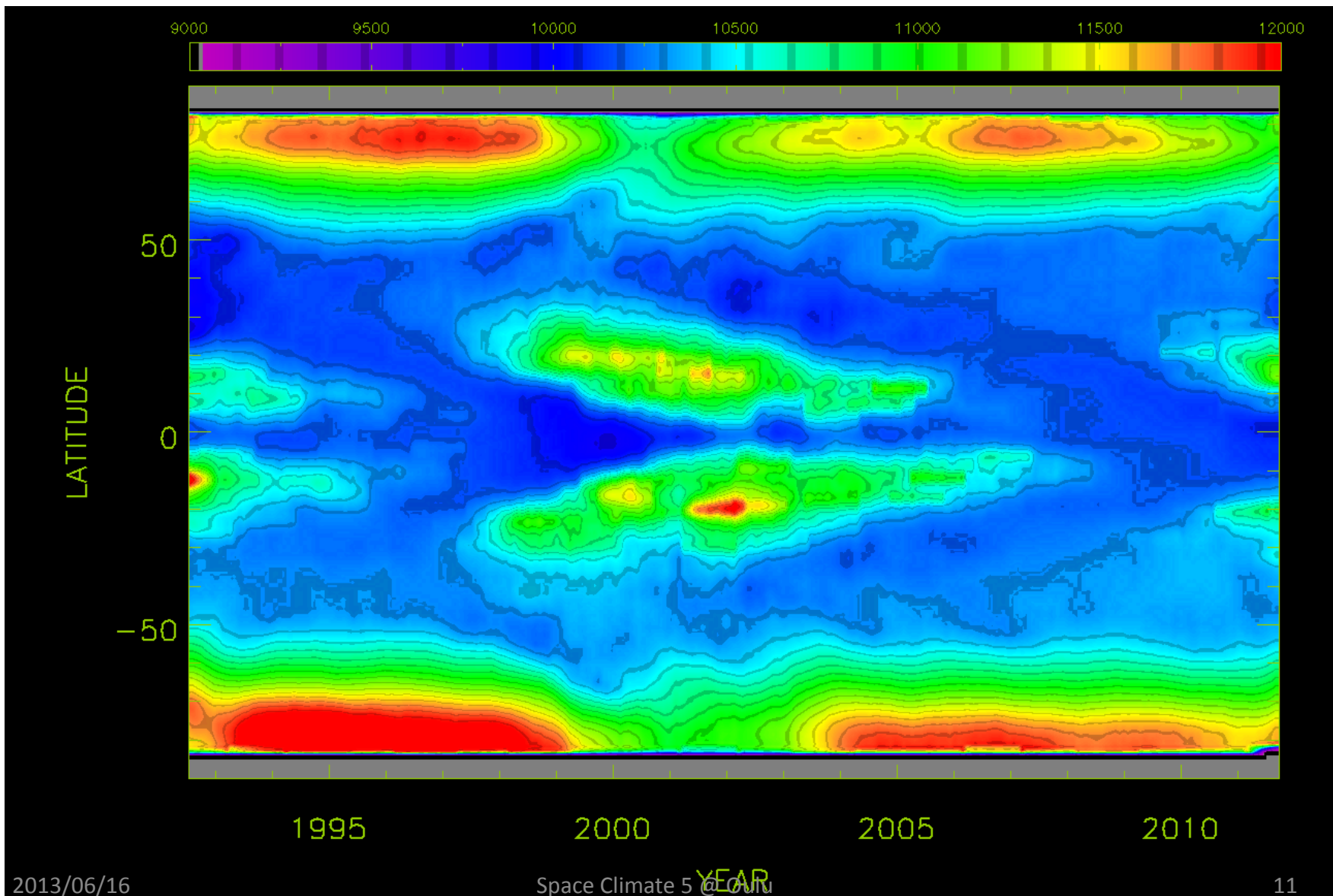


Carrington
Rotation Maps
(260)

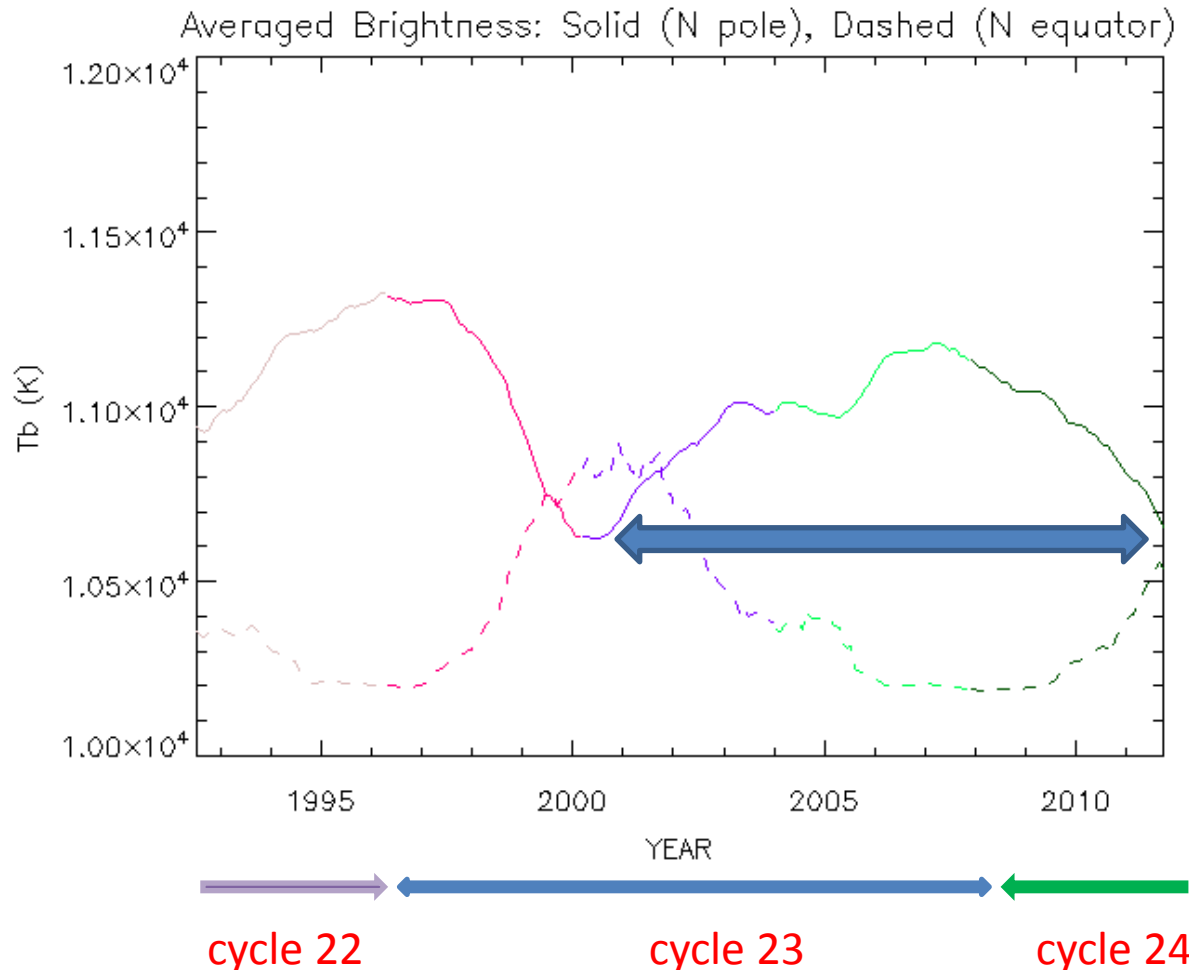


Radio Butterfly
Diagram

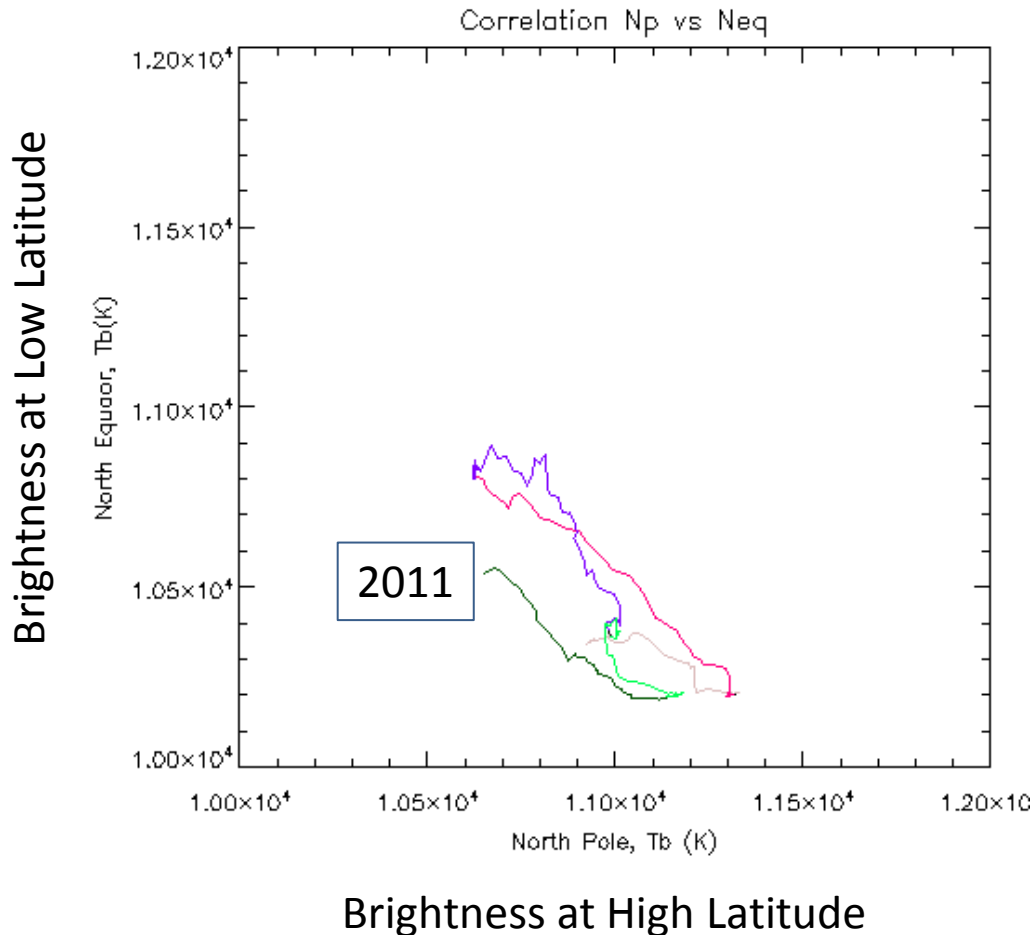
Radio Butterfly Diagram (1992.7-2011.8)



Northern Hemisphere Averaged Brightness (Solid: N55-80, Dotted: N5-35)

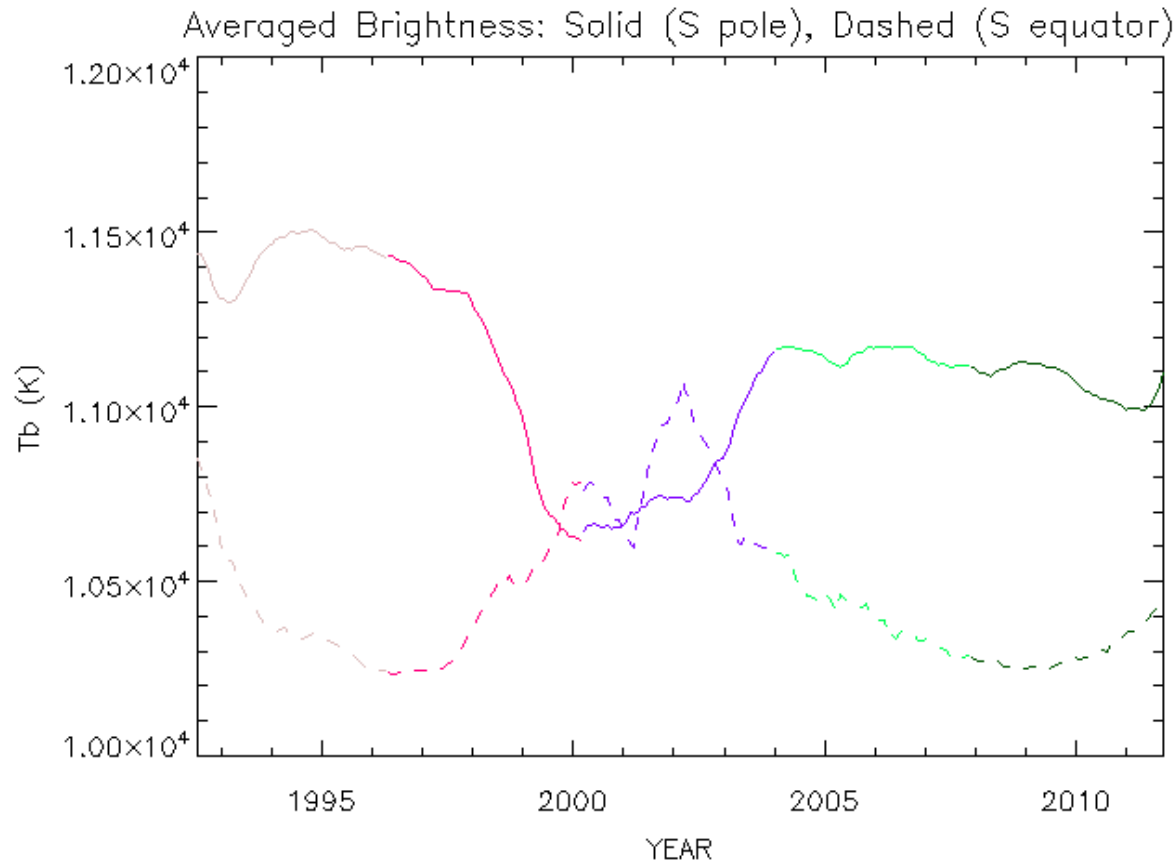


Correlation between High and Low Latitude (Northern Hemisphere)

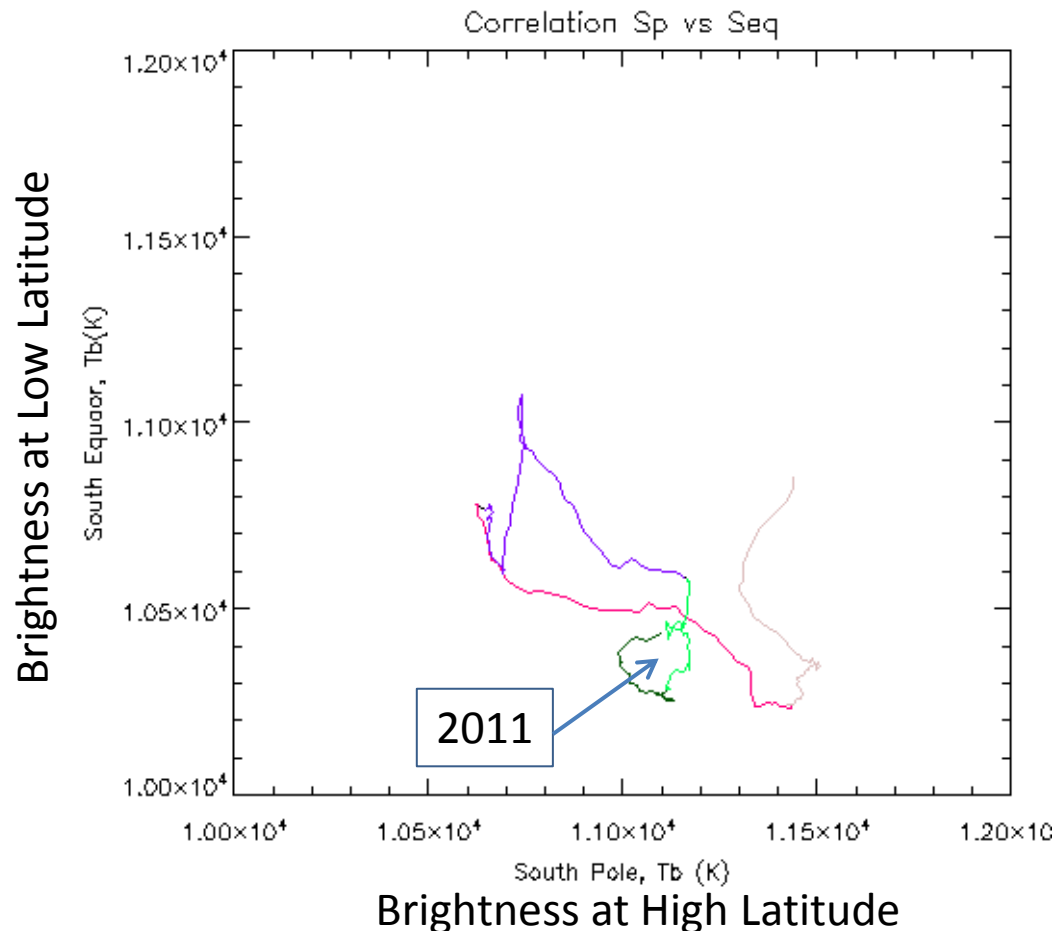


- High Negative Correlation Coeff: -0.83
- 24 cycle (dark green) is shifted toward LL corner.
- Relation between high and low latitudes is kept.

Southern Hemisphere Averaged Brightness (Solid: S55-80, Dotted: S5-35)



Correlation between High and Low Latitude (Southern Hemisphere)



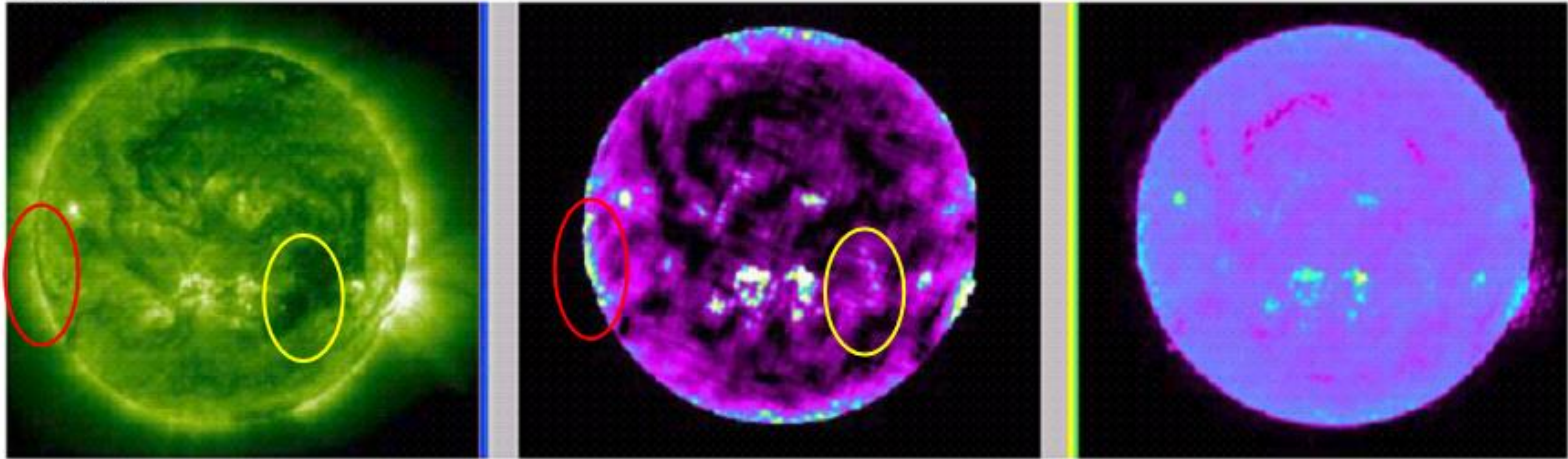
- Weak negative correlation
Coeff: -0.66
- Activities at high and low latitudes are not well synchronized.
- Desynchronization is already existed during cycles 22 and 23.

Why polar regions are bright in microwave

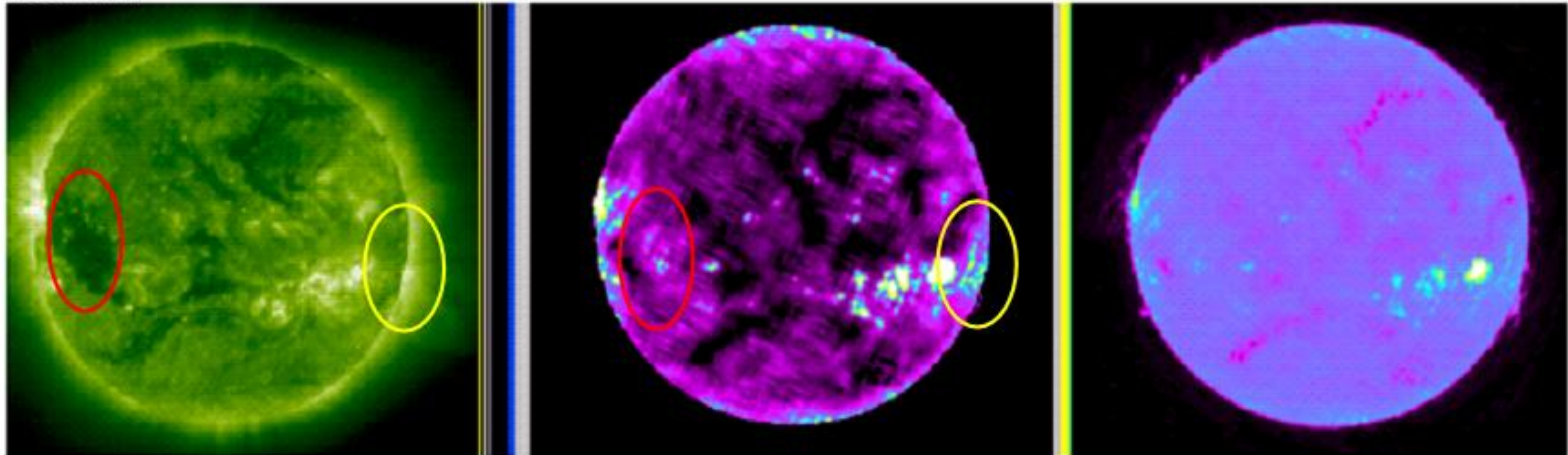
1. Limb brightening effect
 - Due to unknown heating mechanisms of upper atmosphere
2. Coronal hole effect
 - Polar regions are covered by CHs. > enhanced limb brightening
 - During solar max. period > no CHs, dark filaments absorb / suppress limb brightening
3. Magnetic activity effect
 - Good correlation between unipolar mag. field strength and polar brightening (even in low CHs) suggests hotter chromosphere associated with strong mag. field.
 - Enhanced chromospheric heating is needed in open magnetic field region (what mechanism? wave/flare?) proportional to B.
 - Lower coronal temperature in CHs must be due to driving of fast Solar Wind

Coronal Holes everywhere show same behavior as the polar holes

2003/09/10



2003/09/13



Coronal holes are bright in microwaves

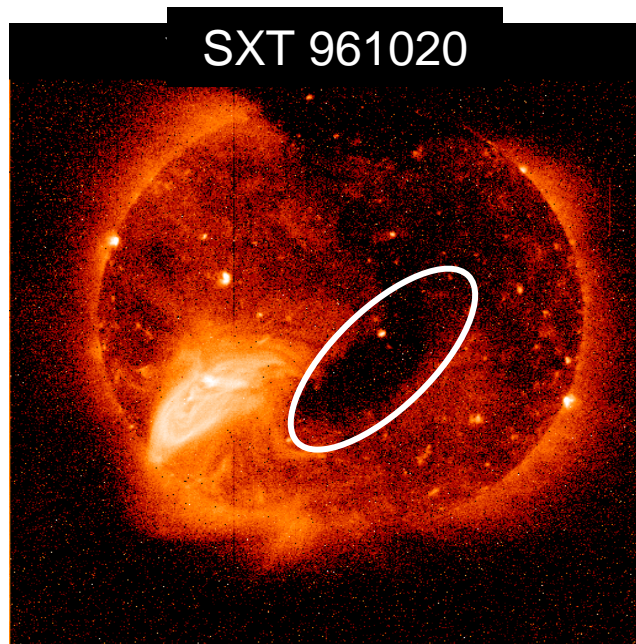
Coronal holes are bright in the frequency range 15-80 GHz (polar & low-latitude)

Quiet-sun emission at 17 GHz comes from the chromosphere

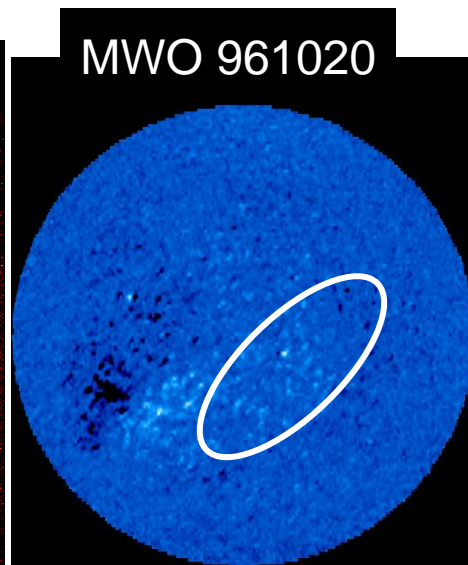
Microwave enhancement is due to different physical conditions in the Chromosphere beneath coronal holes (hotter than quiet sun)

(See Gopalswamy et al., 1999 for a review)

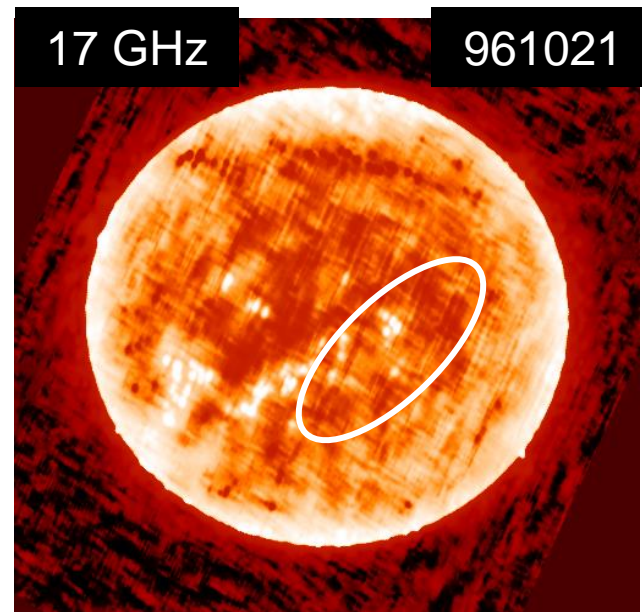
Here we study the solar-cycle variation of the 17 GHz brightness in polar coronal holes



Dark in X-rays



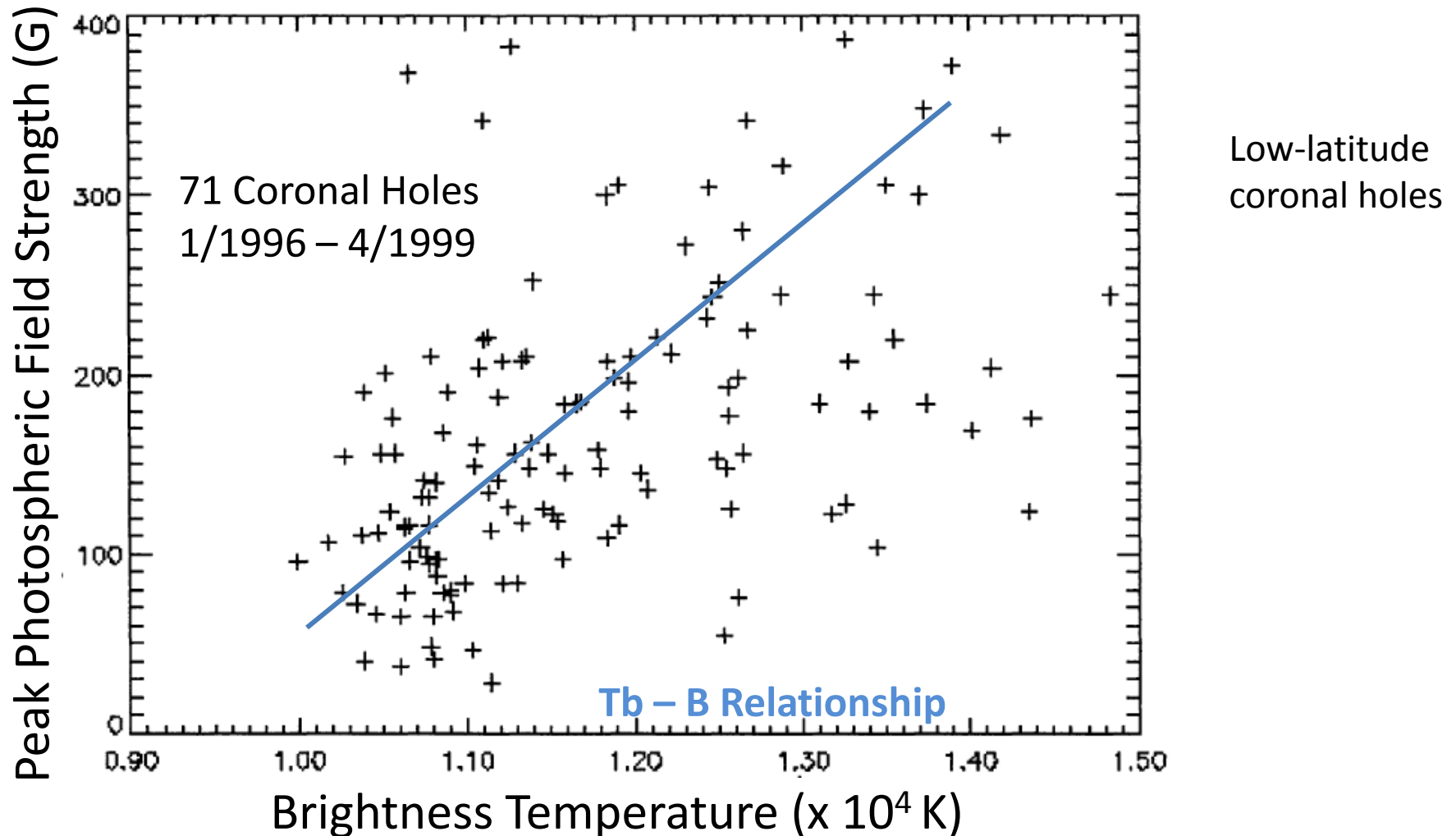
Enhanced unipolar B



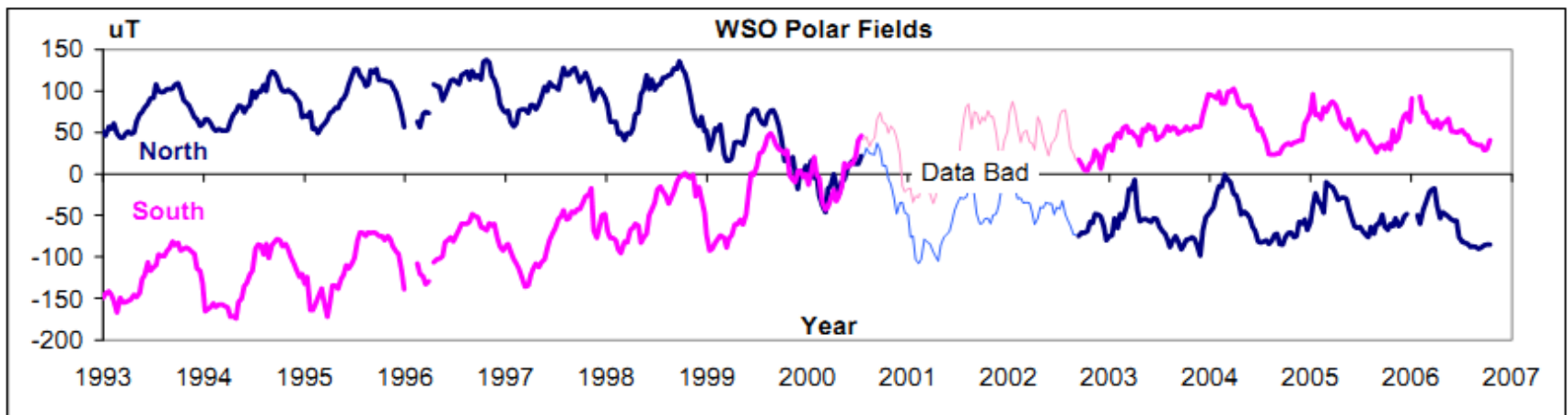
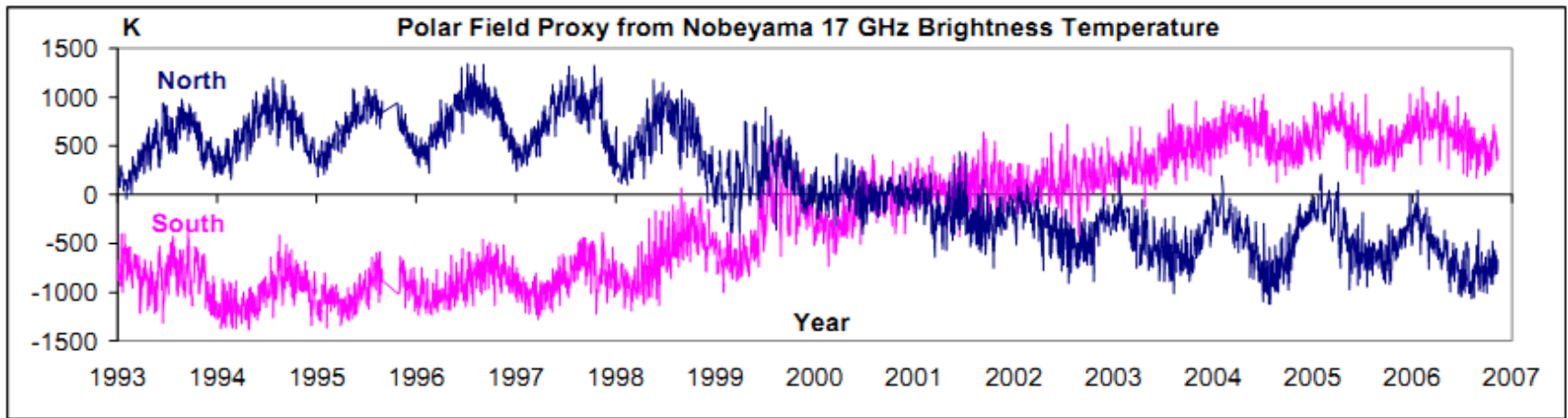
Bright in Microwaves

From Gopalswamy, 2008 JASTP

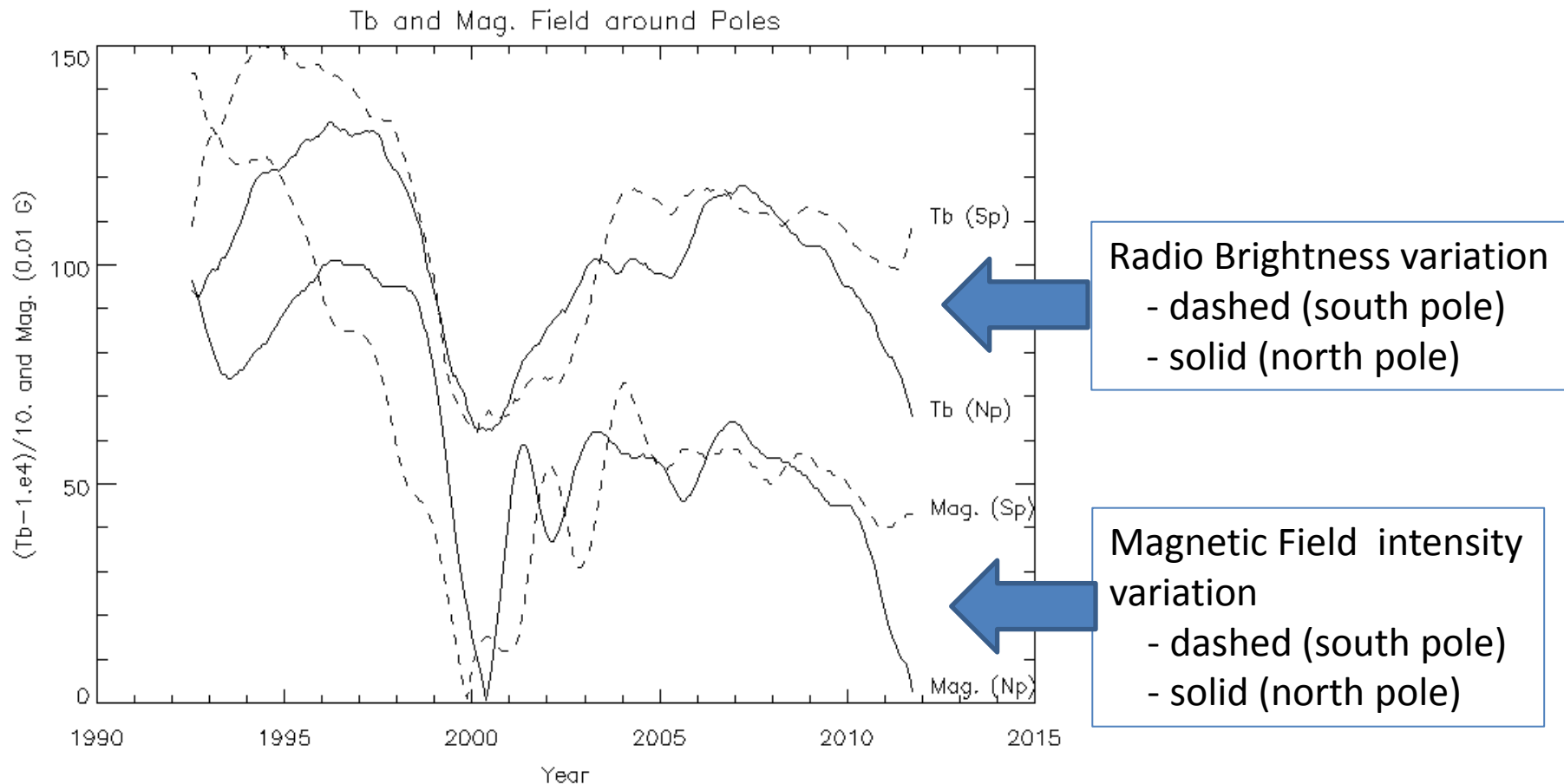
CH Brightness Temperature and underlying photospheric field strength



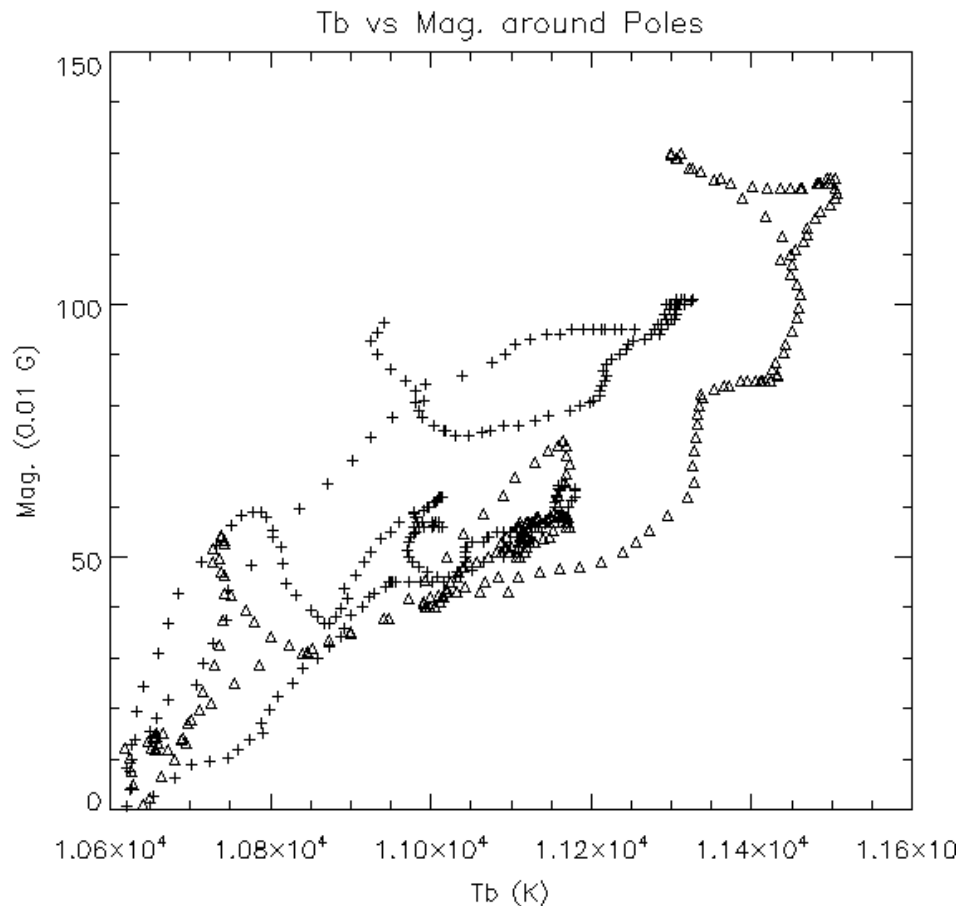
Excess T_b over 10,800K, signed according to WSO polar field sign



Variations of Polar Radio Brightness and Polar Magnetic Field Intensity



Correlation between radio brightness and mag. field strength at polar region



- + : Np、Δ : Sp
- Corr. Coeff. = 0.86
 - North : 0.84
 - South : 0.89
- Radio brightness at polar regions is a good indicator of polar magnetic field, even though physical mechanisms are quite different.

AR Soft X-ray Flux \propto magnetic flux (Φ) (coronal heating) (not $\iint B^2 ds$)

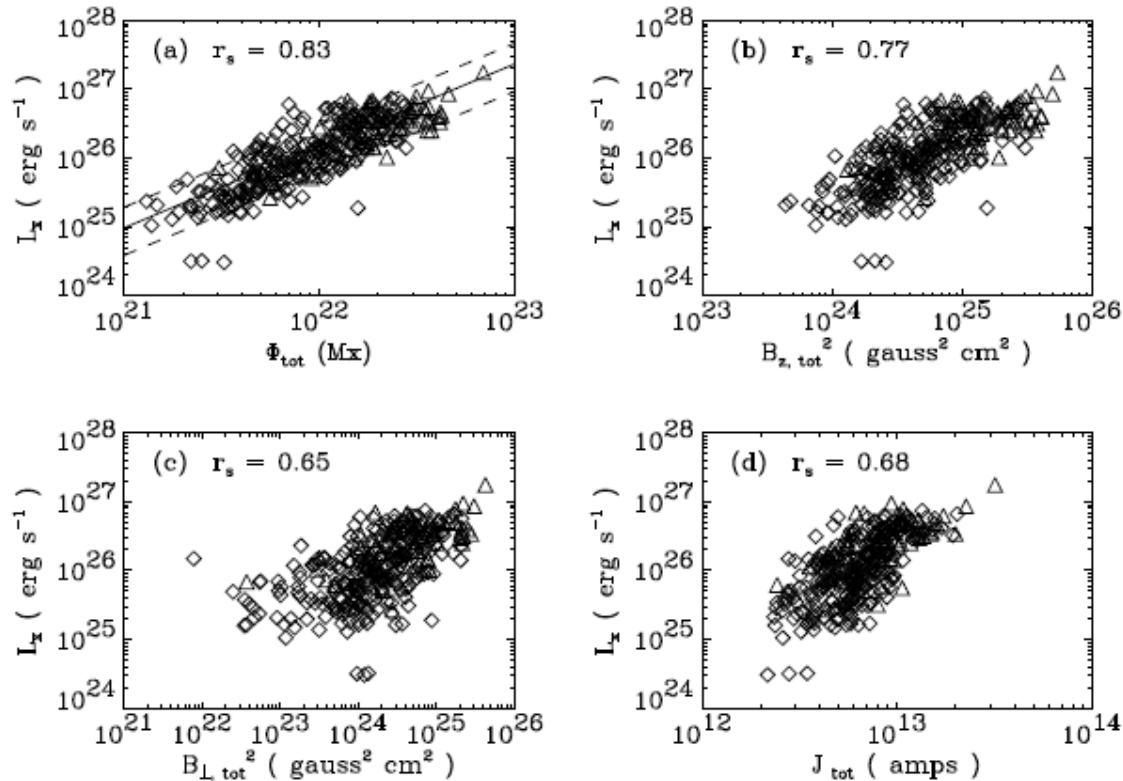
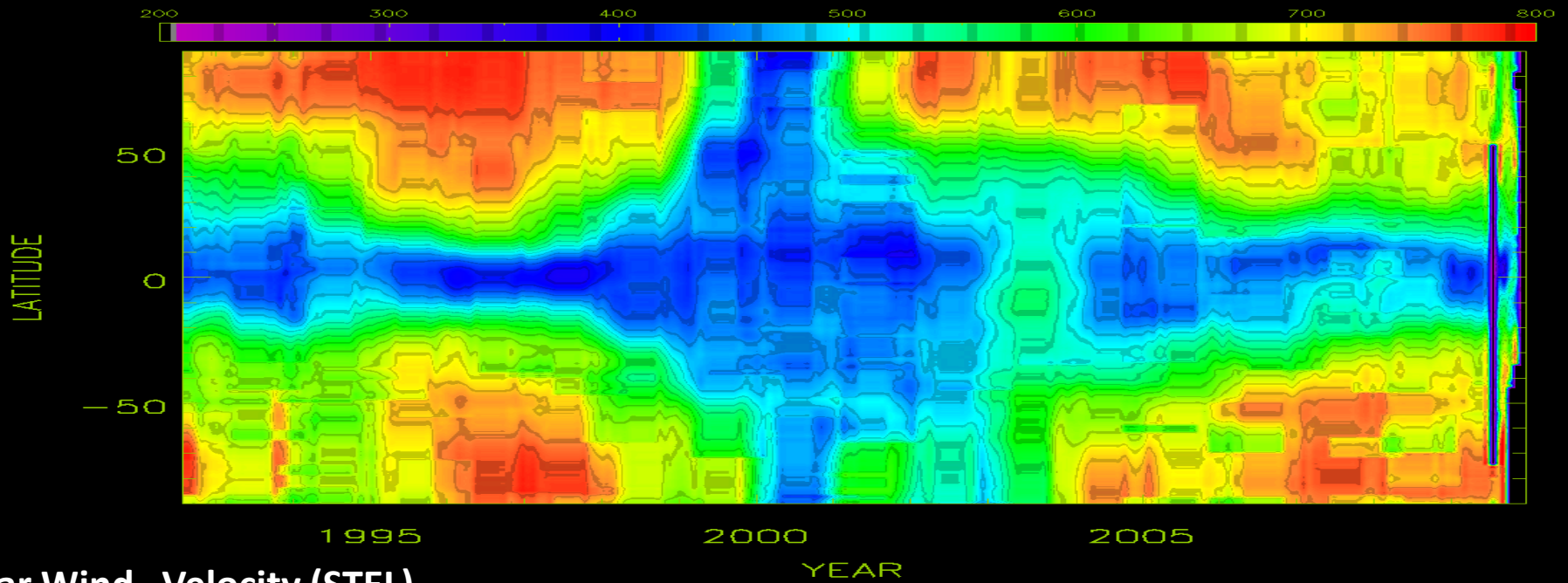
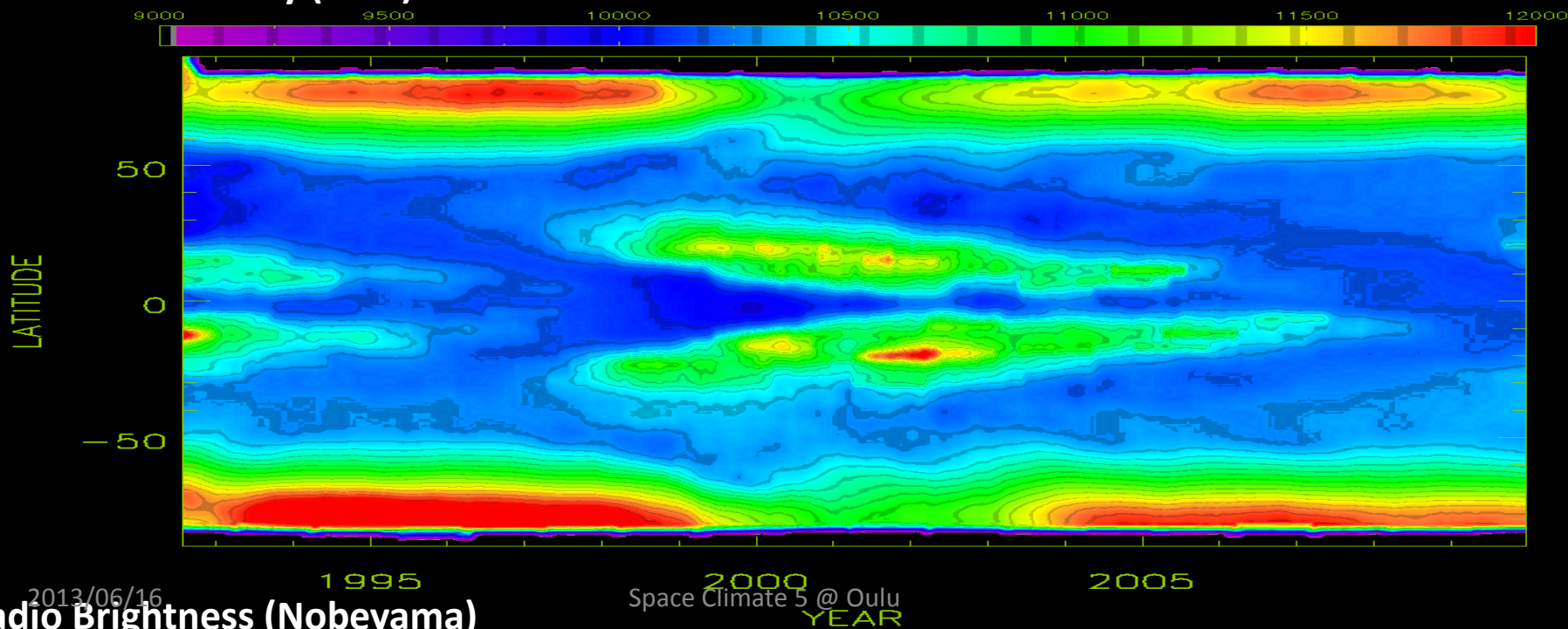


FIG. 2.—Scatter plots of X-ray luminosity versus the four global magnetic quantities Φ_{tot} , $B_{z, \text{tot}}^2$, $B_{\perp, \text{tot}}^2$, and J_{tot} . The Spearman correlation coefficients for these cases are listed with each panel. The power-law relationship $L_x \sim \Phi_{\text{tot}}^{1.19}$ is shown (solid line) along with a band encompassing 80% of the data points (dashed lines). Triangles denote undersampled magnetograms, and diamonds denote critically sampled magnetograms.

Fisher et al. (1998)



Solar Wind Velocity (STEL)



Radio Brightness (Nobeyama)

Summary - 1

1. A radio butterfly diagram is synthesized from daily radio images taken by Nobeyama Radioheliograph for nearly 20 years.
2. Correlation study of averaged brightness variations at low (5 – 35 deg.) and at high (55 – 80 deg.) latitudes shows good anti-correlation (c.c.=-0.83) in the northern hemisphere. In the Southern hemisphere, correlation is rather poor (c.c.=-0.66).
3. Radio brightness excess at both poles during activity minimum 22/23 was roughly half that of 23/24.
4. Global solar activity seems to be in an anomalous state:
 - Desynchronization between North and South hemisphere
 - Desynchronization between high and low latitude activities in the southern hemisphere
 - Weak solar activity maximum of Cycle 24 (first peak in the Northern hemisphere)
5. Radio imaging observation can play important roles for studies of the global solar activity.

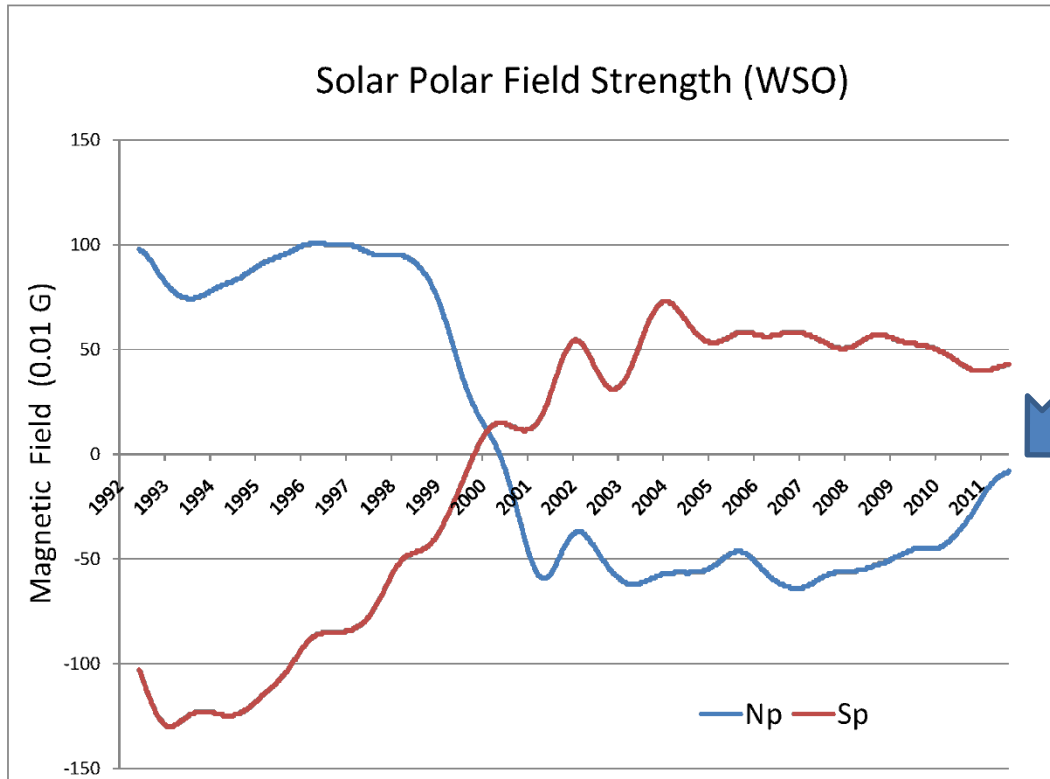
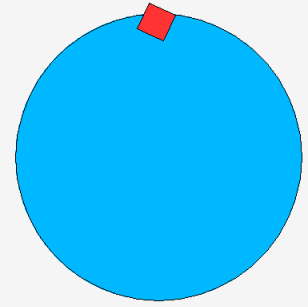
Summary - 2

6. Enhanced chromospheric heating in unipolar open magnetic field regions

- Good correlation between magnetic field strength in polar CHs (and also at low latitude) and microwave brightness suggests enhanced chromospheric heating associated with unipolar strong magnetic flux.
- This is a strong constraint to coronal / chromospheric heating mechanisms (wave, nano-flares or others)
- Observations and a model in enhanced magnetic field region are needed of polar regions: heating the chromosphere and driving the fast solar wind.

END

3.1 WSO polar field 20nHz filtered



- Polar field strength during 23/24 min. was roughly half that of during 22/23 min.
- Polarity reversal corresponds to activity maximum in the Northern hemisphere.

Polar Brightening and Solar Wind

K. Shibasaki (NSRO/NAOJ),
K. Fujiki, and M. Tokumaru
(STEL/Nagoya-U))

Solar Wind Speed Measurement using Interplanetary Scintillation by STEL/Nagoya U.

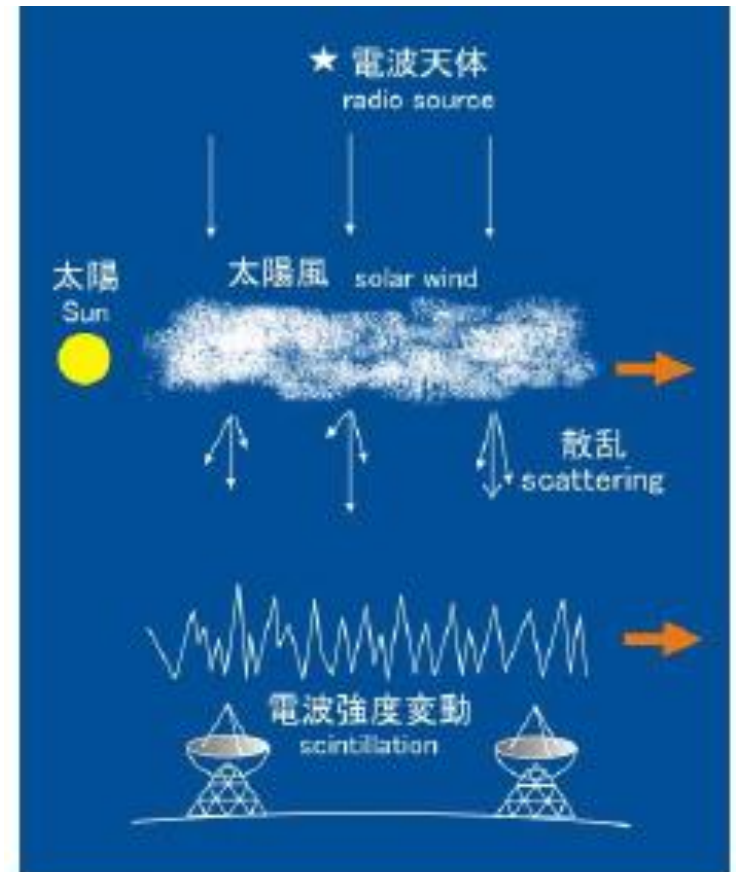
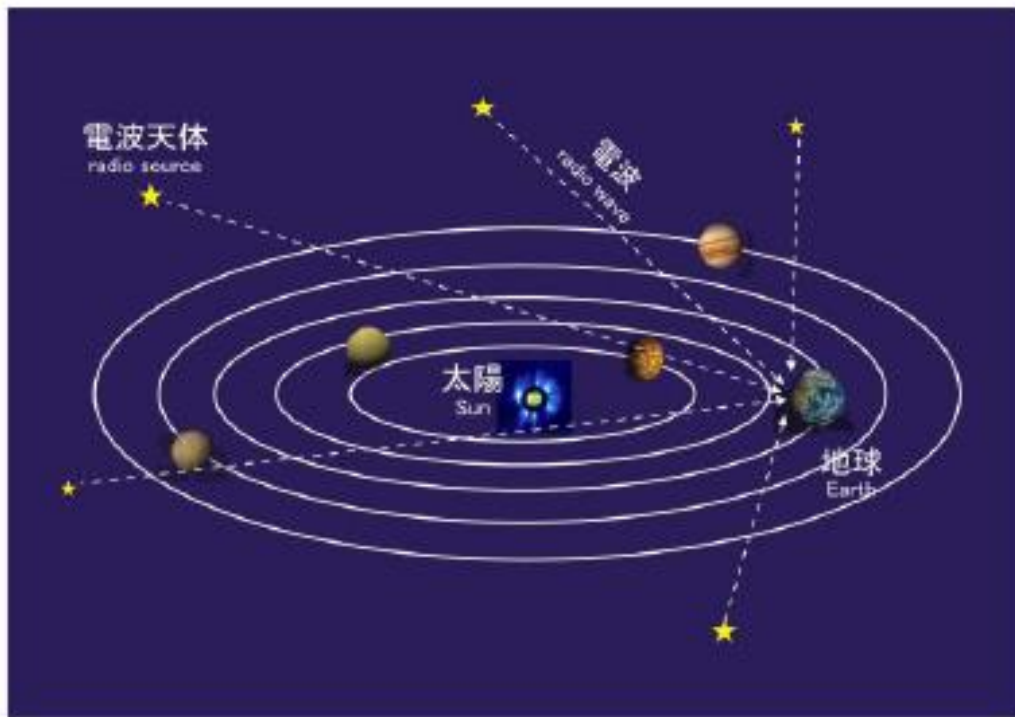
Four stations at Fuji, Toyokawa Sugadaira and Kiso construct four-antenna system, which is fully dedicated to ground-based solar wind observations. The routine-based solar wind observations have been carried out using the interplanetary scintillation method.

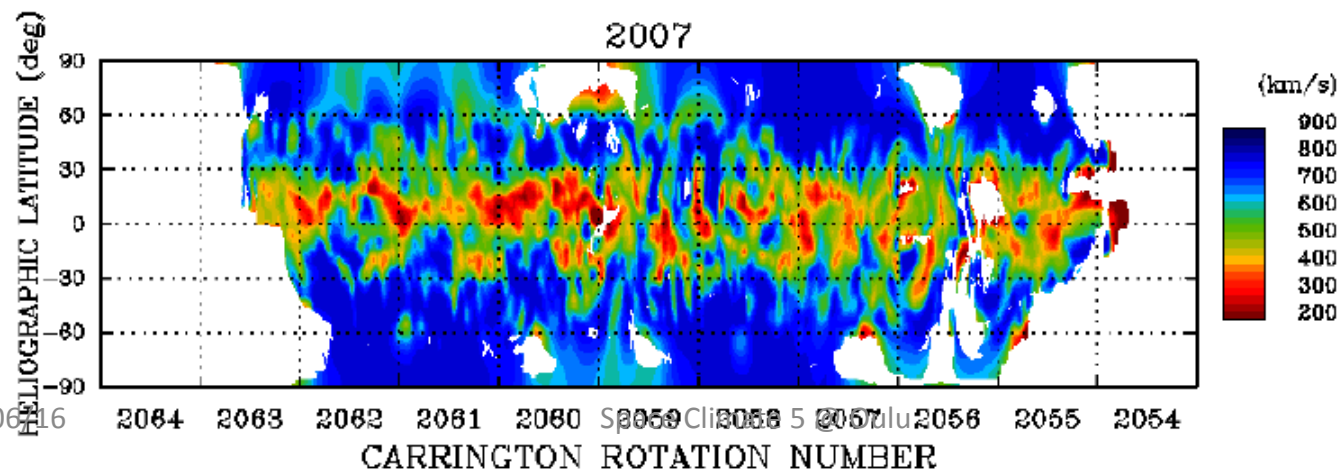
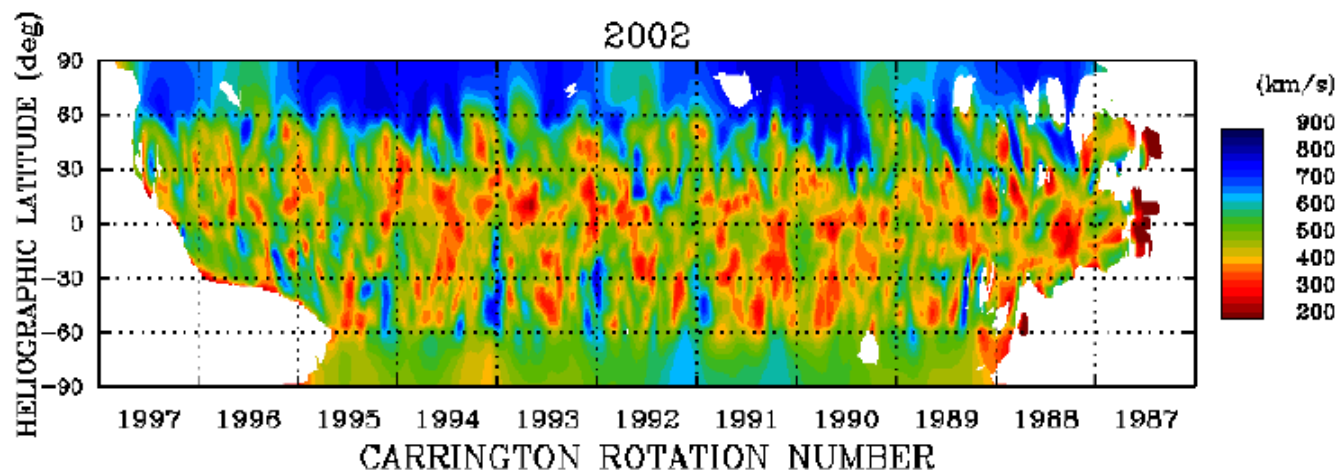
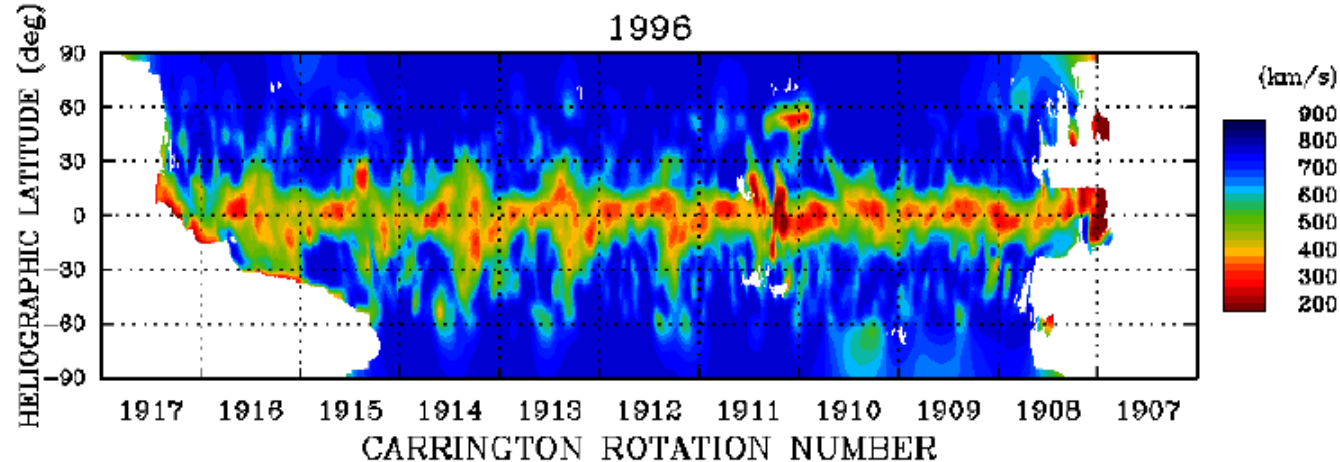


太陽風観測4点システムの観測点の配置。

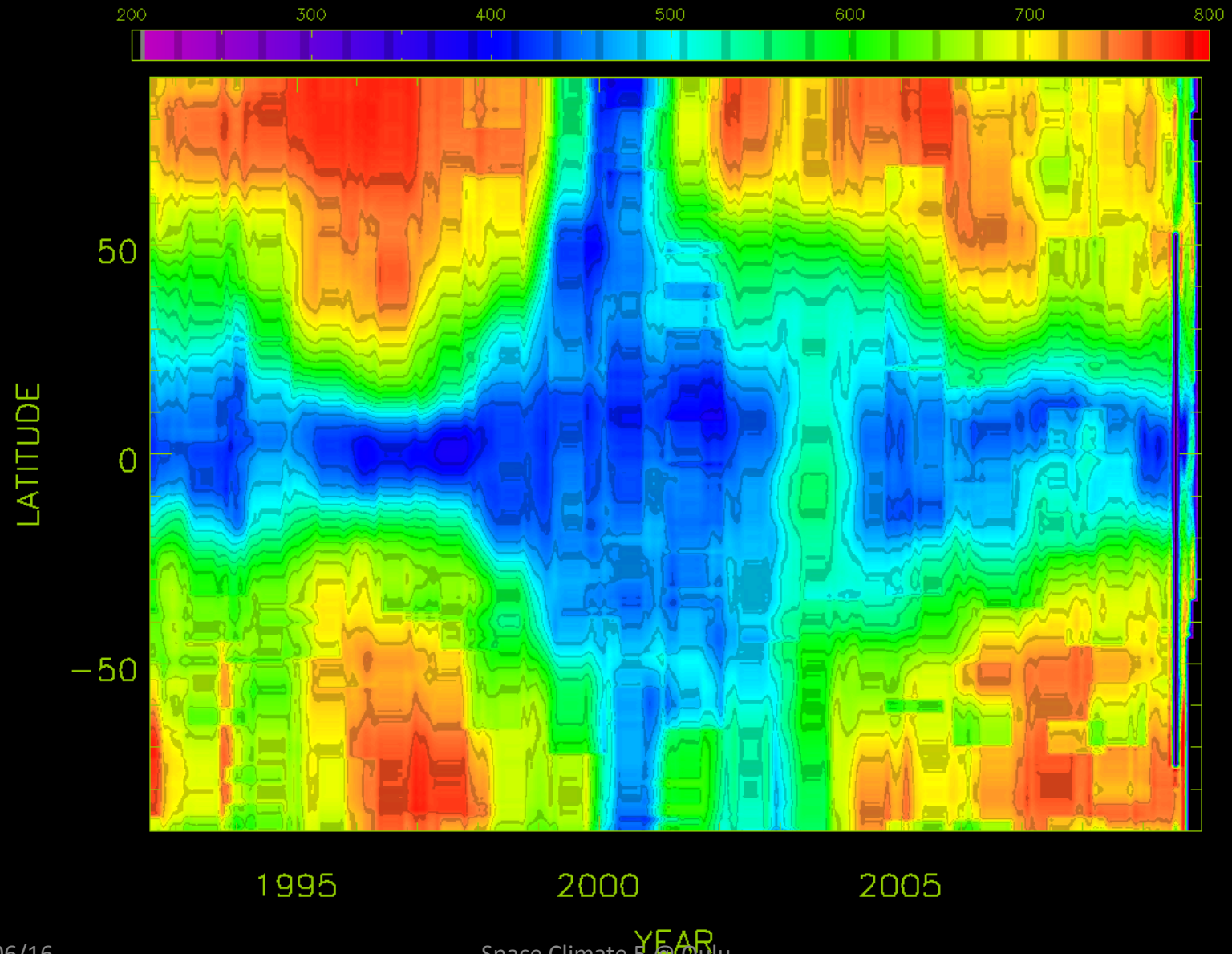
Geographical arrangement of four-antenna system.

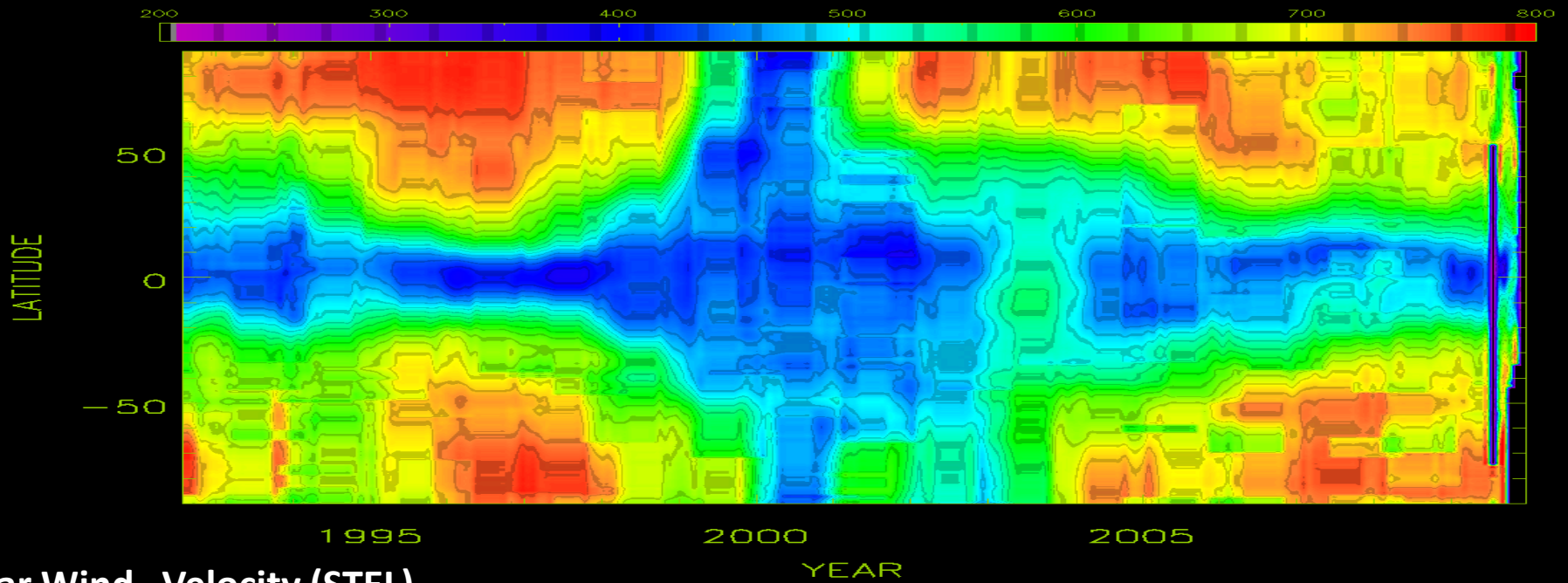
Principle of Solar Wind Speed Measurements



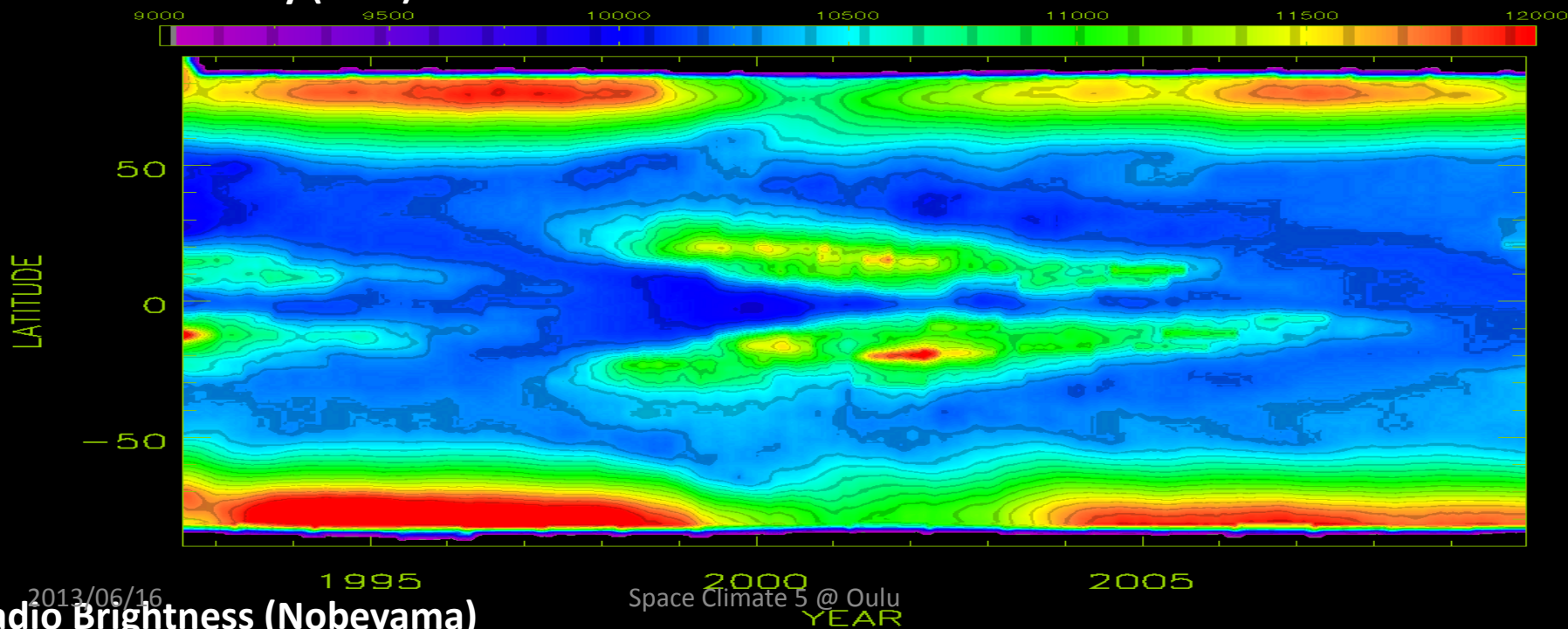


Solar Wind Speed



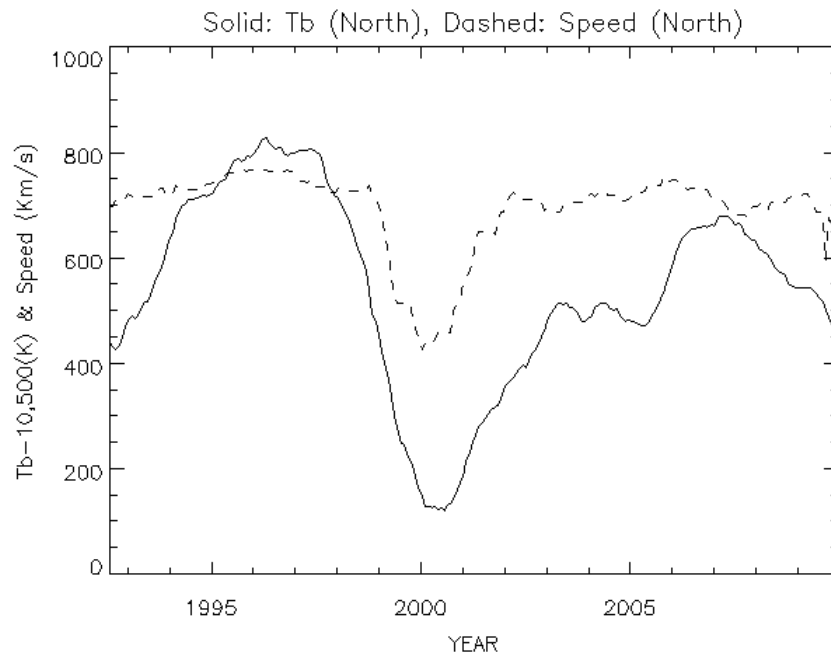


Solar Wind Velocity (STEL)



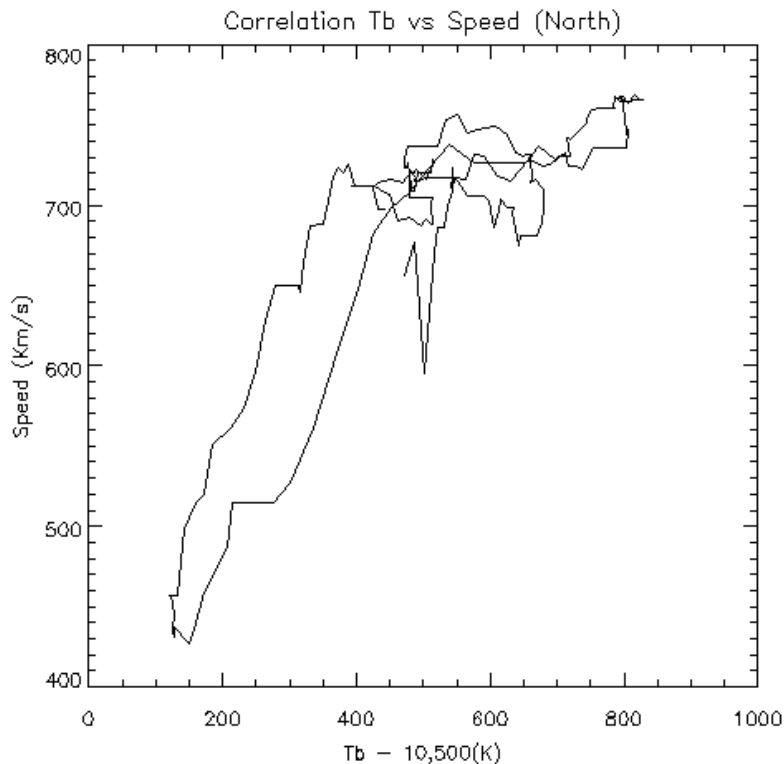
Radio Brightness (Nobeyama)

Northern High Latitude Brightness and Solar Wind Speed



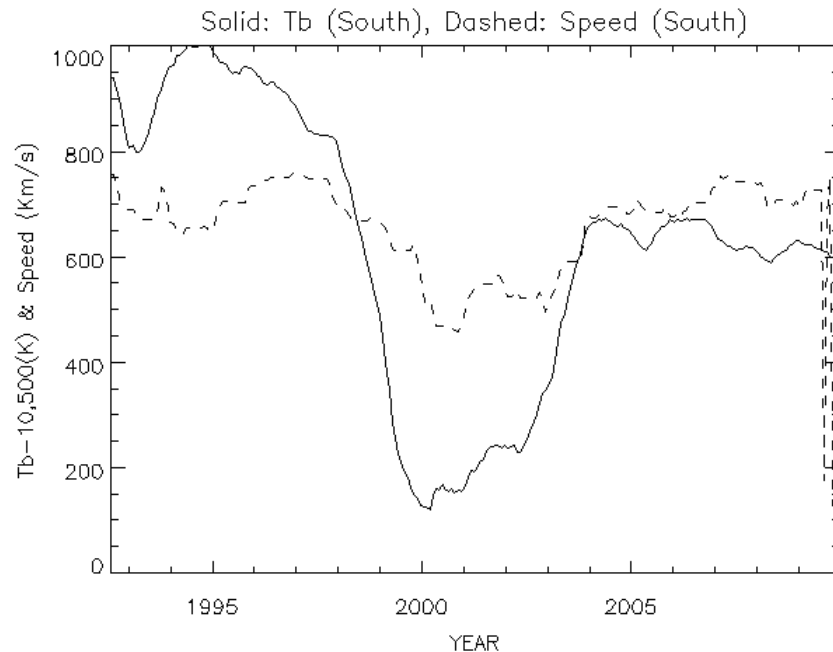
- N55~N80 averaged radio brightness (Tb – 10,500K, solid) and solar wind speed (km/s, dotted)

Correlation between radio brightness and solar wind speed at northern high latitude



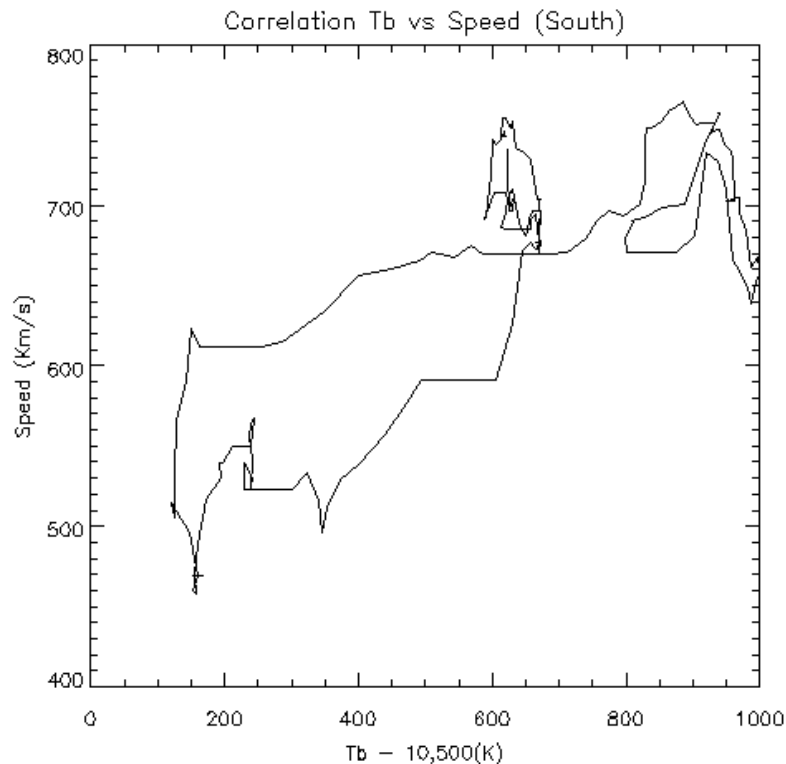
- Correlation Coeff. = 0.83
- Wind speed is nearly constant (750 km/s) at $Tb \geq 11,000$ K

Southern High Latitude Brightness and Solar Wind Speed



- S55~S80 averaged radio brightness (Tb – 10,500K, solid) and solar wind speed (km/s, dotted)

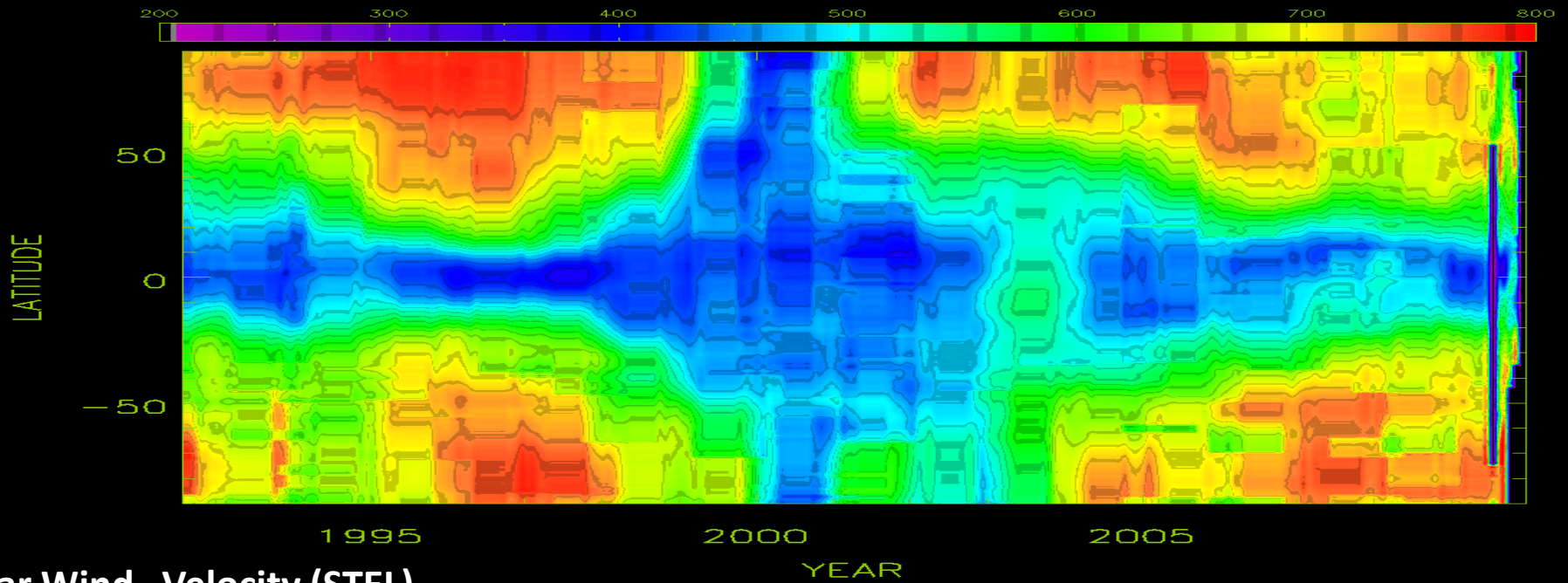
Correlation between radio brightness and solar wind speed at southern high latitude



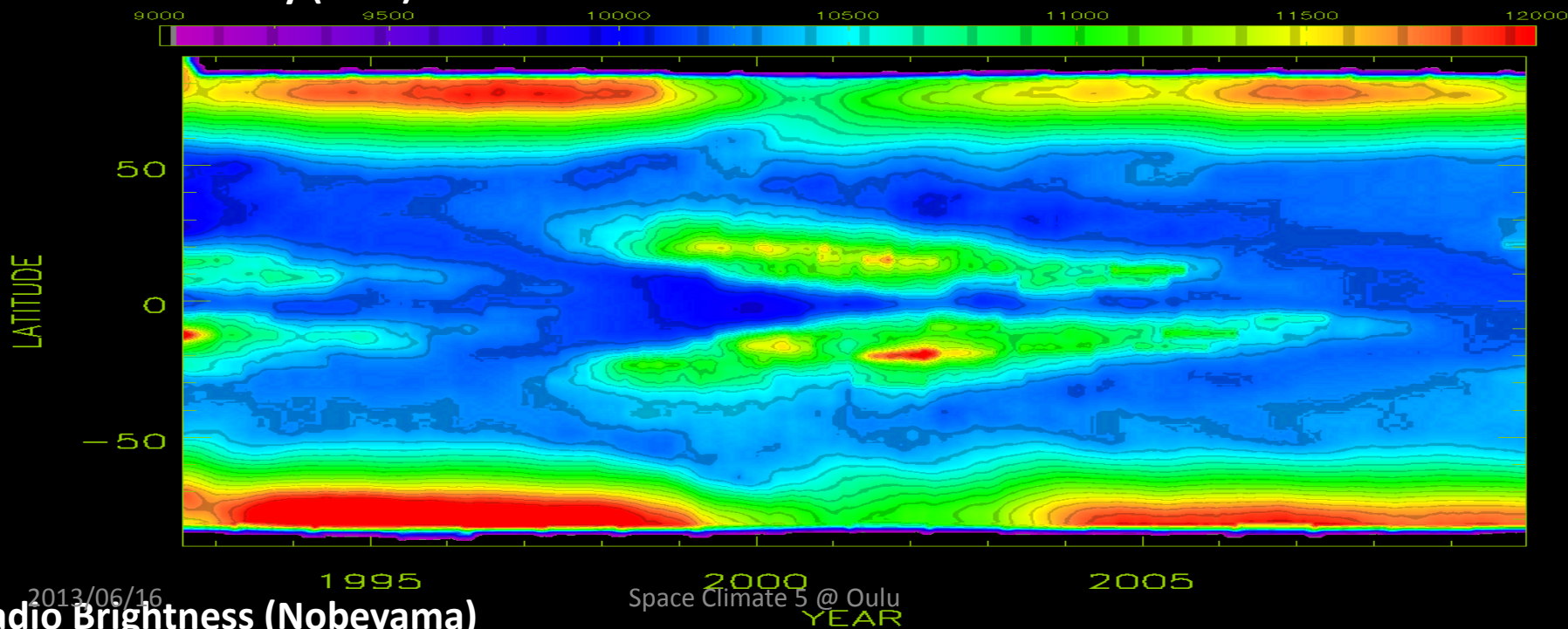
- Correlation Coeff. = 0.79
- Less clear relation (Tb – speed) compared to the northern hemisphere

Why solar wind speed and radio brightness show so good correlation at high latitude

- Both radio brightness and solar wind speed depends on polar field
 - Radio brightness depends on lower atmosphere
 - Solar wind speed depends on higher atmosphere
- During solar maximum period:
 - polar field is weak > closed magnetic field
 - > suppress Tb and inefficient solar wind acceleration



Solar Wind Velocity (STEL)



Radio Brightness (Nobeyama)

Summary

- NoRH observed long-term, global activities of the Sun
 - NoRH characteristics
 - full disk observation
 - robust calibration method (redundant array, good uv coverage for extended quiet Sun disk (position, brightness))
 - proper frequency selection of 17 GHz for polar activity obs.
 - long and steady operation for 20 years
- We need further observations to study the current anomalous condition of global solar activity, not only to understand solar activity itself but also its influence to the interplanetary space and to the earth upper atmosphere.

17 GHz Solar Radius by Selhorst et al.

THE BEHAVIOR OF THE 17 GHz SOLAR RADIUS AND LIMB BRIGHTENING IN THE SPOTLESS MINIMUM XXIII/XXIV

C. L. SELHORST¹, C. G. GIMÉNEZ DE CASTRO², A. VÁLIO², J. E. R. COSTA³, AND K. SHIBASAKI⁴

¹ IP&D-Universidade do Vale do Paraíba-UNIVAP, São José dos Campos, SP, Brazil; caius@univap.br

² CRAAM, Universidade Presbiteriana Mackenzie, São Paulo, SP, Brazil

³ CEA, Instituto Nacional de Pesquisas Espaciais, São José dos Campos, SP, Brazil

⁴ NoRH, Nobeyama Radioheliograph, Japan

Received 2011 February 22; accepted 2011 April 5; published 2011 May 25

THE ASTROPHYSICAL JOURNAL, 734:64 (3pp), 2011 June 10

SELHORST ET AL.

Table 1
Brightening Intensity Maxima During Cycles XXII and XXIII

| Pole | Cycle XXII (% above Quiet Sun) | Cycle XXIII (% above Quiet Sun) | Difference (% above Quiet Sun) | Relative Variation (%) |
|-------|-----------------------------------|------------------------------------|-----------------------------------|------------------------|
| North | 16.3 ± 1.5 | 13.7 ± 1.8 | 2.6 ± 2.3 | 16 ± 15 |
| South | 17.5 ± 1.6 | 13.4 ± 1.3 | 4.1 ± 2.1 | 23 ± 11 |

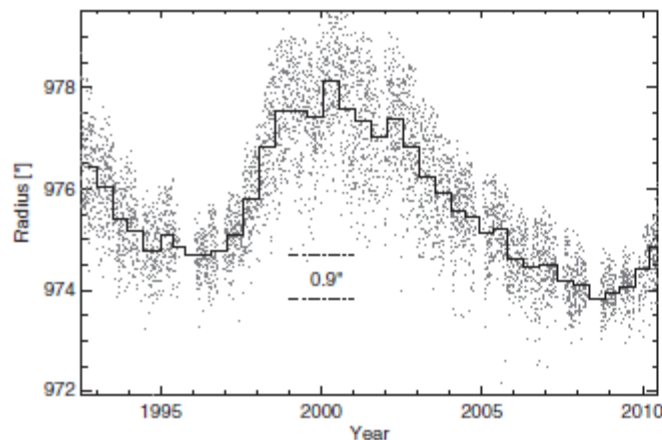


Figure 1. Daily variation of solar radius at 17 GHz (dots) and a 180 days average (thick line). The horizontal dot-dashed lines represent the two minima

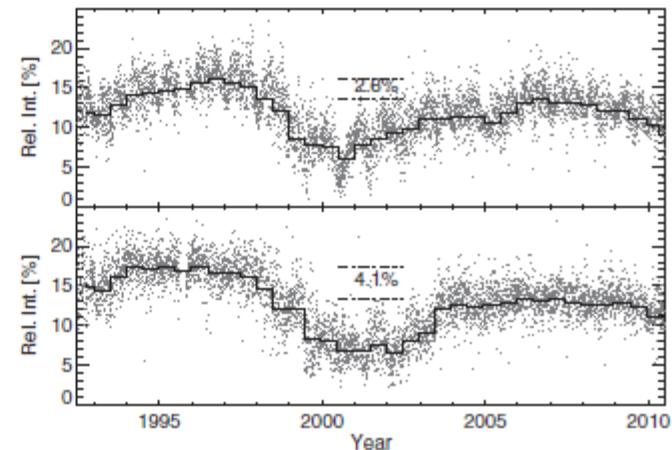


Figure 2. Dots represent the significant daily intensities of the limb brightening at the North (top) and South (bottom) poles. The thick lines are the average taken every 180 days. The horizontal dot-dashed lines represent the average limb brightening intensity during solar minima.